

Determination and Mechanism of Antidiarrheal Chemical Constituents of *Paederia scandens* Determined by HPLC-ESI-MS Integrated with Network Pharmacology

Liwen Ai, Liyang Guo, Weixue Liu, Xuexue Xue, Lulu Li, Zunlai Sheng,* and Chunbo Gao

Cite This: *ACS Omega* 2023, 8, 28834–28845

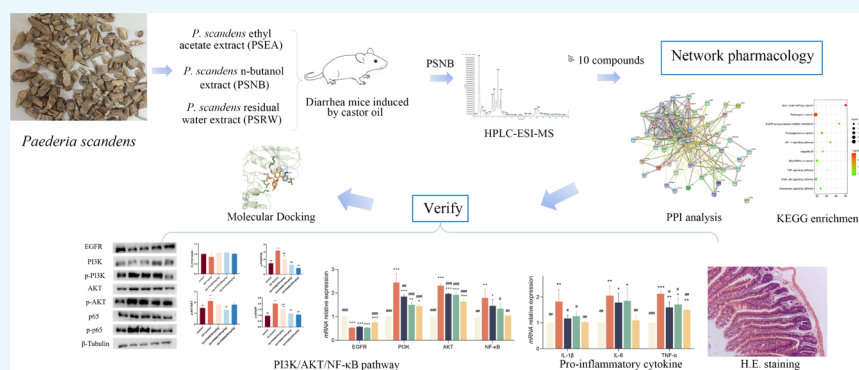
Read Online

ACCESS |

Metrics & More

Article Recommendations

Supporting Information



ABSTRACT: *Paederia scandens* is a natural medicinal plant that is widely used for its various pharmacological effects including antiviral, antitumor, anti-inflammatory, and antibacterial activities. However, there is no scientific evidence to support its antidiarrheal effect. In this study, the antidiarrheal activity of *P. scandens* was evaluated using several validated models. By using HPLC-ESI-MS in conjunction with a network pharmacology approach, the possible antidiarrheal mechanisms of *P. scandens* active fragments were studied, and they were subsequently verified in a mouse model of diarrhea. Finally, utilizing molecular docking, active compounds that might have antidiarrheal properties were hypothesized. The results show that the main antidiarrheal part of *P. scandens* has 10 chemical components in the *n*-butanol fraction (PSNB). The key targets of PSNB and diarrhea, EGFR, AKT1, and PIK3CA, were screened by network pharmacology analysis. And the mechanism of PSNB in the treatment of diarrhea may be highly related to the EGFR tyrosine kinase inhibitor resistance and PI3K/AKT signaling pathway. Besides, through the qRT-PCR and western-blot experiments, it was found that PSNB could inhibit the gene expression of proinflammatory factors by reducing the protein expression of AKT1 and PI3K and regulating the NF- κ B signaling pathway in mice. In addition, asperuloside, paederoside, paederoside acid methyl ester, and 6'-O-E-feruloylmonotropein have better docking energies than other chemical components in PSNB with EGFR, AKT1, and PIK3CA. In conclusion, the main antidiarrheal active site of *P. scandens* is the *n*-butanol site. PSNB may exert an antidiarrheal effect by regulating the PI3K/Akt/NF- κ B signaling pathway. Among them, asperuloside, paederoside, paederoside acid methyl ester, and 6'-O-E-feruloylmonotropein may be the active ingredients that exert an antidiarrheal effect.

1. INTRODUCTION

Diarrhea, the more frequent passing of abnormally liquid or unformed stools, is also a major cause of morbidity and mortality in developing countries, especially in children. The causes of diarrhea are complex and can be caused by viruses, bacteria, parasites, and drugs. Studies have shown that diarrhea is accompanied by a certain inflammatory response,¹ so antibiotics are currently used for treatment, including gentamicin, enrofloxacin, penicillin, streptomycin, etc.,² but problems such as antibiotic residues and some bacterial resistances are becoming more and more serious, and antibiotic therapy is found to cause diarrhea, that is, antibiotic-associated diarrhea, when antibiotics are used to

treat other diseases.³ Therefore, there is a need to develop safe and effective alternative treatment strategies for diarrhea. Additionally, WHO has also launched a program to combat diarrhea that makes use of conventional herbal remedies. The use of natural substances as antidiarrheal medications, such as extracts of herbs and spices, is gaining popularity. These

Received: June 2, 2023

Accepted: July 12, 2023

Published: July 24, 2023



chemicals could occasionally be less harmful and more specialized than those made through synthesis. For a long time, many traditional Chinese medicines have been used to treat diarrhea with significant clinical efficacy.^{4–6}

Paederia scandens (Lour.) Merri. is a Rubiaceae plant, which has a wide medicinal history in China, Japan, Korea, and Taiwan, and the extract of *P. scandens* (PSE) displays antiviral, antitumor, anti-inflammatory, and antimicrobial activities.^{7–9} It is used in China and Vietnam to treat toothache, chest pain, hemorrhoids, spleen inflammation, rheumatoid arthritis, and bacillary dysentery.¹⁰ Iridoid glycosides are the major constituents of *P. scandens*, including asperuloside, paederoside, and scanderoside.¹¹ Recently, studies have shown that iridoid glycosides in *P. scandens* can reduce uric acid, and anti-inflammatory and immunomodulatory properties play a protective role against renal injury in UAN rats.¹² Previous studies have shown that iridoid glycosides, morroniside, and loganin in *Cornus officinalis* can treat colitis by blocking the STAT3/NF- κ B pathway.¹³ Gentiopicroside, as a secoiridoid compound isolated, can reduce the expression levels of TNF- α , IL-1 β , IL-6, iNOS, and COX-2 to exert an anti-inflammatory effect on experimental acute colitis.¹⁴ At present, some studies show that *P. scandens* can be used as protection against kidney damage in UAN rats. To the best of our knowledge, there are no reports on the antidiarrheal effect of *P. scandens*.

In this work, we used a variety of validated models to assess the antidiarrheal activity of the *P. scandens* aqueous extract. Moreover, the active fragment was further determined, and its main constituents were identified by HPLC-ESI-MS. Then, we used network pharmacology to have the predictive key components and potential targets of *P. scandens* in its antidiarrheal effect and the mice diarrhea model to verify these targets to provide a scientific basis for the clinical application of this drug in the future treatment of diarrhea.

2. RESULTS

2.1. Acute Toxicity Study. *P. scandens* aqueous extract (PSAE) was given to three distinct groups of mice in graduated doses of 2000, 4000, and 5000 mg/kg, respectively. Up to 48 h after the administration of the plant extract, the animals were monitored for any changes in behavior or deaths. In all test groups, the extract treatment did not result in any significant behavioral changes or animal deaths.

2.2. Antidiarrheal Activity. **2.2.1. Inhibition of Castor Oil-Induced Diarrhea.** To verify the antidiarrheal effect of PSAE, one experiment was performed using the castor oil-induced diarrhea model. As shown in Table 1, the data indicated that castor oil could make mice produce loose feces

Table 1. Effect of PSAE on Castor Oil-Induced Diarrhea in Mice^a

group	dose (mg/kg)	onset of diarrhea (min)	mean number of wet/loose feces in 4 h	percent inhibition (%)
control		103 \pm 37	7.5 \pm 2.4	
loperamide	5	92.7 \pm 27.8	3.5 \pm 1***	53.3
PSAE	100	100.8 \pm 18.7	6 \pm 1.9	13.3
PSAE	200	96.7 \pm 40	5 \pm 2.4*	33.3
PSAE	400	92.2 \pm 26.5	4.1 \pm 1.2**	44.4

^aData are presented as the mean \pm SD. The symbol for the significance of differences between the control group and another group: * P < 0.05, ** P < 0.01, *** P < 0.001.

within 4 h, and compared with the control group and loperamide, on diarrhea animals, with a strong inhibitory effect. Compared with the strong inhibitory effect of loperamide on diarrhea animals, 200 and 400 mg/kg could significantly reduce the number of loose feces (P < 0.05), but not as strongly. PSAE at the further reduced levels of 100 mg/kg had little or no effect at all on castor oil-induced diarrhea.

2.2.2. Castor Oil-Induced Transit in Mice. To evaluate the effect of PSAE on intestinal motility in mice, we used charcoal propulsion experiments as an evaluation of intestinal transit. The results indicated that in mice, PSAE (200 and 400 mg/kg) significantly decreased the gastrointestinal distance traveled by the charcoal meal compared to the control (P < 0.05), but the extract (100 mg/kg) group showed no significant inhibition. The intestine inhibition induced by loperamide (5 mg/kg) was 30.0%, which was significantly higher than the 18.7% intestinal inhibition produced by the highest dose of PSAE (400 mg/kg). (Table 2).

Table 2. Effect of PSAE on Gastrointestinal Motility in Mice^a

group	dose (mg/kg)	movement of the charcoal meal (%)	inhibition (%)
control		84.02 \pm 2.1	
loperamide	5	58.80 \pm 5.3***	30.0
PSAE	100	77.52 \pm 8.8	11.0
PSAE	200	71.08 \pm 2.3***	15.4
PSAE	400	68.34 \pm 6***	18.7

^aData are presented as the mean \pm SD. The symbol for the significance of differences between the control group and another group: *** P < 0.001.

2.2.3. Effect on Castor Oil-Induced Enteropooling. As shown in Table 3, the present results showed that castor oil-

Table 3. Effect of PSAE on Castor Oil-Induced Enteropooling in Rats^a

group	dose (mg/kg)	volume of intestinal content (mL)	inhibition (%)
control		3.32 \pm 0.3	
loperamide	5	1.47 \pm 0.1***	55.7
PSAE	100	3.0 \pm 0.24**	9.6
PSAE	200	2.83 \pm 0.14***	14.7
PSAE	400	1.8 \pm 0.24***	45.8

^aData are presented as the mean \pm SD. The symbol for the significance of differences between the control group and another group: ** P < 0.01, *** P < 0.001.

induced fluid accumulation in rats was significantly reduced by PSAE, the reduction being progressively greater the higher the pretreatment level (P < 0.01, P < 0.001) with inhibition rates of 9.6, 14.7, and 45.8%, respectively.

2.3. Screening of the Antidiarrheal Fraction. Castor oil-induced diarrheal mice were pretreated with the fractionated PSAE fractions (50, 100, and 200 mg/kg) to further explore the antidiarrheal effect of PSAE. As shown in Table 4, the data showed that loperamide and *P. scandens* *n*-butanol extract (PSNB) (200 mg/kg) significantly reduced the number of loose stools compared to the control group (P < 0.001). PSNB (100 mg/kg) and *P. scandens* ethyl acetate extract (PSEA) (200 mg/kg) had an inhibitory effect on diarrhea animals (P < 0.01), while *P. scandens* residual water extract

Table 4. Effect of PSAE on Castor Oil-Induced Diarrhea in Mice^a

group	dose (mg/kg)	mean number of wet/loose feces in 4 h	percent inhibition (%)
control		8.83 ± 2.1	
loperamide	5	3.83 ± 1.2***	56.6
PSEA	50	8.33 ± 1.2	5.7
PSEA	100	7.5 ± 1.0	15.1
PSEA	200	6.67 ± 0.8**	24.5
PSNB	50	7.67 ± 1.4	13.2
PSNB	100	6.33 ± 1.2**	28.3
PSNB	200	5 ± 0.9***	43.4
PSRW	50	8.67 ± 1.5	1.9
PSRW	100	8.17 ± 1.2	7.5
PSRW	200	7.33 ± 1.5	17.0

^aData are presented as the mean ± SD. The symbol for the significance of differences between the control group and another group: ** $P < 0.01$, *** $P < 0.001$.

(PSRW) and other doses of PSNB and PSEA pretreatment had no inhibitory effect on diarrheal mice.

2.4. Identification of Constituents in the Active Fraction of PSNB by HPLC-ESI-MS. The chemical profiles of PSNB were explored by HPLC-ESI-MS both in positive and negative ionization modes. The total ion chromatogram of PSNB is shown in Figure 1; literature data and reference standards were applied to identify the chemical constituents from the chemical profile of PSNB. As shown in Table 5, a total of 10 compounds, including 9 iridoids and 1 coumarin, were identified. The relevant data for the identification of these compounds are shown in Table 5. Among them, 6'-O-E-feruloylmonotropein was identified by the comparison of experiments by Kim et al.¹⁵ Methyl deacetylasperulosidate and paederosidic acid methyl ester were confirmed by the comparison with the reference standard Ren,¹⁶ and other compounds were confirmed by the fragmentation pathways of these compounds. The MS spectra of each compound are shown in Supporting Information Figure S1.

2.5. Network Pharmacology Analysis Results.

2.5.1. Target Recognition Results. Diarrhea-related genes were retrieved using the DisGeNET database, and a total of 632 targets were screened. Targets were predicted for 10 key compounds through the Swiss database, and a total of 350 targets were obtained after deduplication. The compound targets and diarrheal disease targets were intersected, and 57 common target genes were screened. The proportional Venn diagram was plotted using <http://www.bioinformatics.com.cn>, a free online platform for data analysis and visualization, and the results are shown in Figure 2A.

2.5.2. Construction and Analysis of the PPI Network. The 57 common target genes were input into the String platform (<https://string-db.org/>) to obtain the PPI interaction diagram (Figure 2B). The PPI results were exported as a simple textual data format (.tsv), and the TSV file was imported to Cytoscape 3.9.1 to acquire the network diagram of the target interaction (Figure 2C). In addition, EGFR, TNF, AKT1, ALB, CD4, ERBB2, STAT3, IL2, KDR, PIK3CA, and MAPK1 represented the crucial targets based on the highest degree, which are the mutual core of the network.

2.5.3. Gene Ontology (GO) and Kyoto Encyclopedia of Genes and Genomes (KEGG) Enrichment Analyses. We imported 57 targets into the DAVID 6.8 database and plotted

the GO function and KEGG signal pathway with $P < 0.01$. The characteristics of diarrhea-related targets were investigated by GO enrichment and KEGG pathway enrichment analysis. The GO function represents three aspects of biology: molecular functions (MFs), biological processes (BPs), and cellular components (CCs). GO enrichment analysis showed that target genes were mostly related to the BPs of protein phosphorylation, positive regulation of protein phosphorylation, regulation of cell adhesion, etc. The enriched MF ontologies were dominated by phosphotransferase activity, with an alcohol group as the acceptor, kinase activity, protein kinase activity, and so on. The cytoplasm was the smallest proportion in CC analysis (Figure 3A). Finally, KEGG analysis revealed that the co-target gene could affect multipathways, including non-small cell lung cancer, EGFR tyrosine kinase inhibitor resistance, HIF-1 signaling pathway, PI3K/AKT signaling pathway, etc. (Figure 3B).

2.5.4. Network Construction. To further explore the preventive effect and mechanism of *P. scandens* and its extracts on the diarrhea system, a map of *P. scandens* *n*-butanol fraction compounds and their related targets for diarrhea prevention, as well as the KEGG signaling pathway network map of co-target genes, was constructed (Figure 3C,D).

2.6. Effects of PSNB on Diarrheal Mice. **2.6.1. Histopathological Analysis.** To assess histological changes in diarrheal mice and the protective effect of PSNB, we assessed the structure of the mice ileal tissue using H&E staining. As shown in Figure 4, no abnormal changes were observed in the ileal tissue of the control group. The ileum tissue of the mice in the oil control group showed edema of the villus, a small space between the villus, an increased number of lymphocytes, inflammatory infiltration, and mucosal thickness reduction. After PSNB (200 mg/kg) treatment, these pathological changes were markedly reversed, with increased intervillous space and decreased lymphocyte numbers.

2.6.2. PSNB Inhibits Proinflammatory Cytokine Production. To elucidate the anti-inflammatory effect of PSNB on the small intestinal tissue, we detected the mRNA expression levels of TNF- α , IL-1 β , and IL-6. As shown in Figure 5A, the detected gene levels of TNF- α , IL-1 β , and IL-6 indicated that PSNB had an anti-inflammatory effect on diarrheal mice. The study found that there was a significant increase in mRNA expression levels of TNF- α , IL-1 β , and IL-6 in mice with castor oil-induced diarrhea. However, when mice were treated with PSNB, the mRNA expressions of TNF- α , IL-1 β , and IL-6 were significantly reduced in mice receiving high-dose PSNB gavage compared to the oil control group ($P < 0.01$).

2.6.3. Effects of PSNB on the PI3K/Akt/NF- κ B Signaling Pathway and EGFR in Mice with Diarrhea. To further validate the results of the network pharmacology analysis, we examined the effect of PSNB on the PI3K/Akt/NF- κ B pathway in castor oil-induced diarrheal mice. As shown in Figure 5, the detected PI3K/AKT/NF- κ B signaling pathway and EGFR gene levels indicated the therapeutic effect of PSNB on the PI3K/AKT/NF- κ B signaling pathway in diarrheal mice. The results indicated that the expression levels of PI3K, AKT, and NF- κ B mRNA and the protein in castor oil-induced diarrheal mice were significantly increased ($P < 0.01$, $P < 0.001$), the level of EGFR mRNA was significantly decreased ($P < 0.001$), and the protein expression level was down-regulated with no significant difference. After PSNB treatment, the mRNA levels of PI3K, AKT, and NF- κ B were significantly decreased ($P < 0.01$, $P < 0.001$), and the phosphorylation

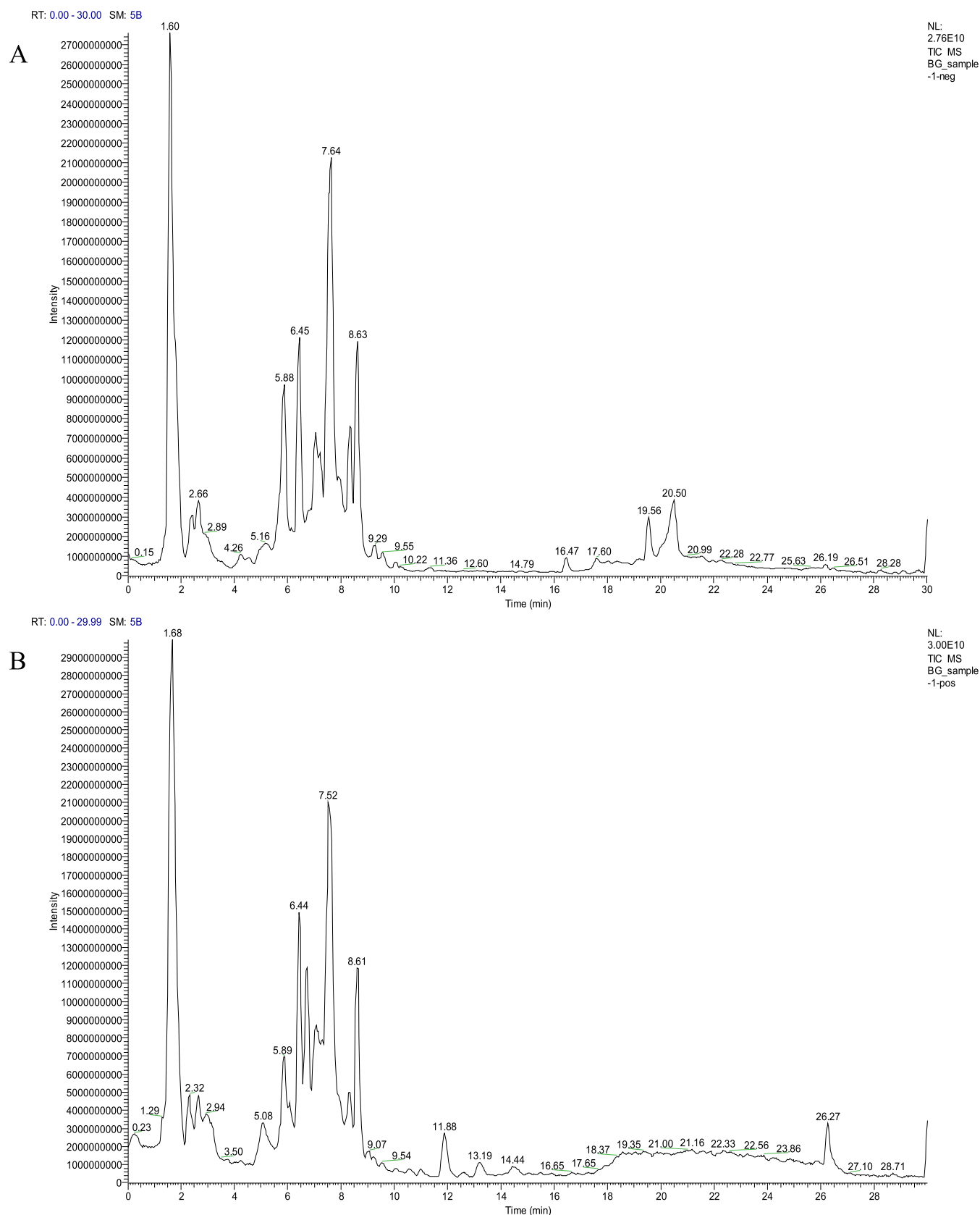


Figure 1. HPLC-ESI-MS total ion chromatograms of PSNB in negative ion mode (A) and positive ion mode (B).

levels of PI3K, AKT, and NF- κ B p65 proteins were significantly downregulated ($P < 0.01$, $P < 0.001$). In conclusion, PSNB can improve castor oil-induced activation

of the PI3K/Akt/NF- κ B signaling pathway in the small intestine of mice, but the activation of the PI3K/AKT/NF- κ B signaling pathway is independent of EGFR.

Table 5. HPLC-ESI-MS Data of the Major Constituents of PSNB

Rt (min)	identification	chemical formula	quasi-molecular ion (m/z)	MS/MS fragments (m/z)
2.38	scandoside	C ₁₆ H ₂₂ O ₁₁	389.10801[M – H] [–]	227.0563[M – H-Glc] [–]
4.26	deacetylasperulosidic acid	C ₁₆ H ₂₂ O ₁₁	389.108[M – H] [–]	227.0563[M – H-Glc] [–]
5.88	methyl deacetylasperulosidate	C ₁₇ H ₂₄ O ₁₁	403.12672[M – H] [–] 449.1292[M + HCOO] [–]	241.07025[M – H-Glc] [–]
6.45	asperulosidic acid	C ₁₈ H ₂₄ O ₁₂	431.12308[M – H] [–]	251.05584[M – H-Glu] [–]
7.01	paederoside	C ₁₈ H ₂₂ O ₁₁ S	447.12932[M + H] ⁺	429.11773[M + H-H ₂ O] ⁺
7.08	cleomiscosin D	C ₂₁ H ₂₀ O ₉	417.11512[M + H] ⁺	399.10889[M + H-OH] ⁺
7.48	asperuloside	C ₁₈ H ₂₂ O ₁₁	413.11283[M – H] [–]	249.06037[M – H-C ₆ H ₁₂ O ₅] [–]
7.67	paederosidic acid	C ₁₈ H ₂₄ O ₁₂ S	463.09466[M – H] [–]	283.03[M – H-Glu] [–]
7.92	6'-O-E-feruloylmonotropein	C ₂₆ H ₃₀ O ₁₄	565.14783 [M – H] [–]	521.20046[M – H-CO ₂] [–]
8.64	paederosidic acid methyl ester	C ₁₉ H ₂₆ O ₁₂ S	523.11363[M + HCOO] [–]	315.0535[M – H-Glc] [–]

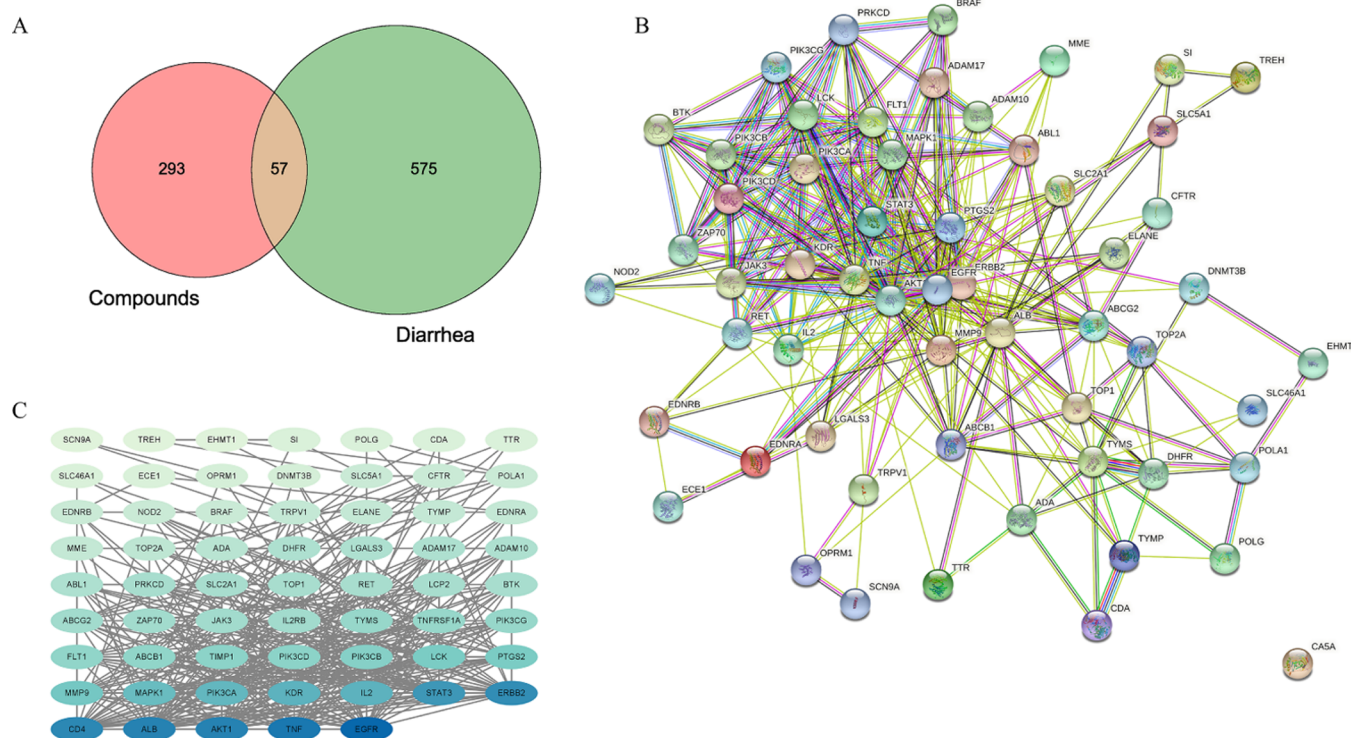


Figure 2. Potential targets of PSNB and diarrhea-related and the PPI network. (A) Venn diagram of PSNB and diarrhea-related targets. (B) PPI network of 57 targets according to the STRING database. (C) PPI network ranked the degree value. The degree value is represented by the color; the darker the color, the higher the degree value.

2.7. Molecular Docking Analysis. In order to further determine the effect of each component on the key targets of diarrhea, through molecular docking analysis, the interaction model of the core target protein and PSNB compounds was determined at the molecular level. A lower binding affinity indicates a more stable binding of the two molecules. In this study, we docked the co-targets (PIK3CA, AKT1, and EGFR) screened by network pharmacology with ten active monomers of PSNB. The results showed that ten compounds had the binding ability to co-targets, among which are asperuloside, paederosidic acid, paederoside, paederosidic acid methyl ester, and 6'-O-E-feruloylmonotropein, and EGFR, AKT1, and PIK3CA protein binding energies are less than -6 kcal/mol, indicating good binding (Table 6). Figure 6 shows the docking results of the five compounds with PIK3CA, AKT1, and EGFR. The results show that the five compounds mainly interact with hydrophobicity (gray dashed line) through hydrogen bonds (blue line), and salt bridges (yellow dashed

line) also play a role when only a small part of the compounds bind to proteins.

3. DISCUSSION

To verify the medicinal value of *P. scandens* on diarrhea, this study aimed to evaluate the antidiarrheal and antisecretory components of the plant extract in mice and to evaluate the possible underlying mechanisms using network pharmacology. In castor oil-induced diarrhea, charcoal propulsion, and intestinal fluid accumulation models, PSAE showed antidiarrheal and antisecretory activities at 200 and 400 mg/kg, similar to the standard antidiarrheal agent loperamide.¹⁷ This inhibitory effect justifies the use of PSAE in traditional medicine and its use as a nonspecific antidiarrheal agent that meets certain criteria for use as an antidiarrheal agent.¹⁸ These criteria include suppression of moist or unformed animal feces and gastrointestinal suppression.

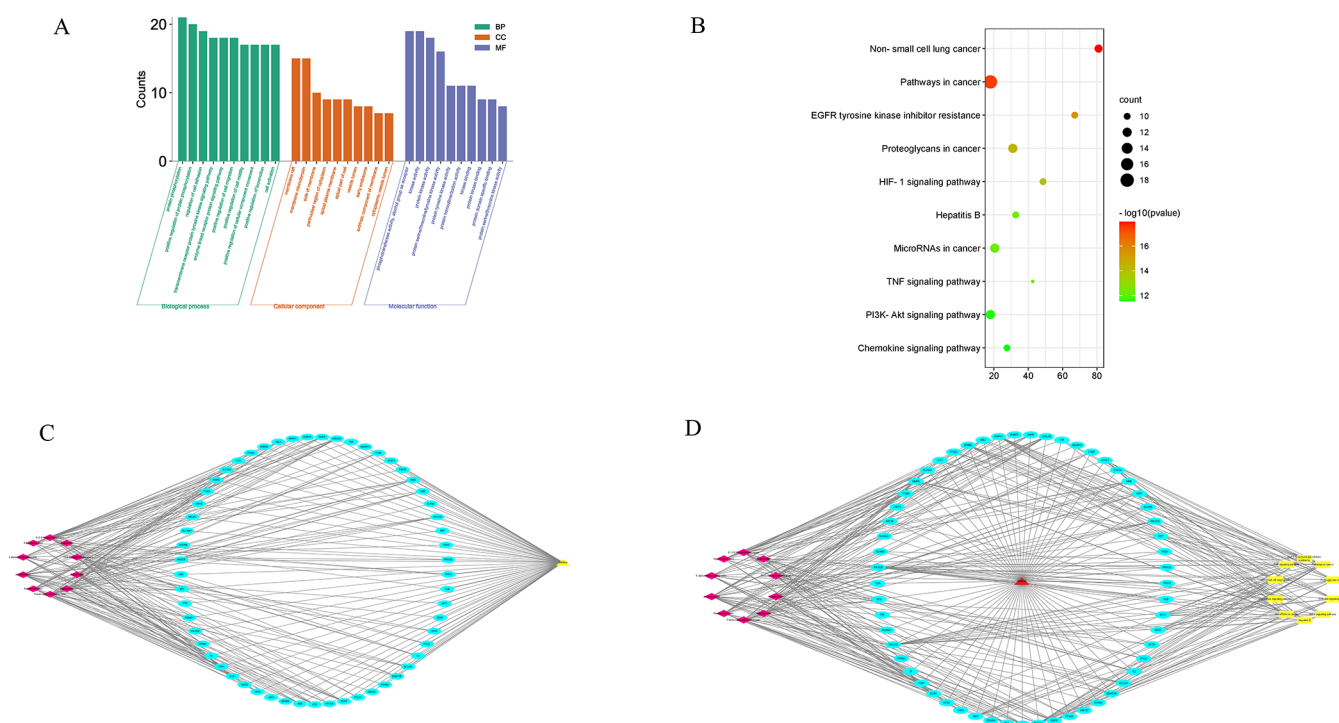


Figure 3. Possible mechanism of PSNB antagonizing diarrhea. (A) GO enrichment and classification diagram of common target genes. (B) KEGG pathway enrichment analysis of key targets. (C) "Compound–target–disease" interaction network diagram. (D) Network PSNB of the key compound–diarrhea target KEGG pathway.

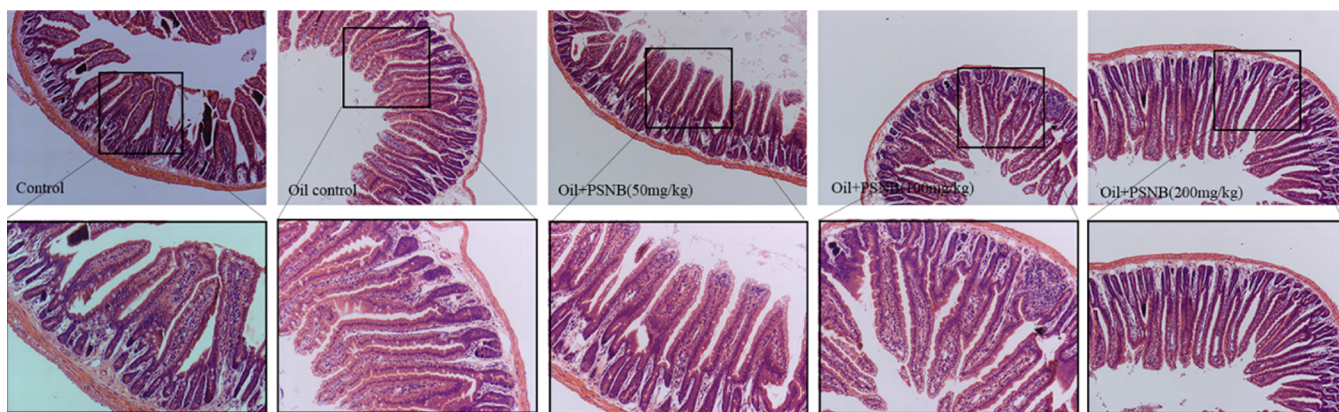


Figure 4. Effects of castor oil and PSNB on ileal histopathology.

After extraction, we found that both the ethyl acetate fraction and the *n*-butanol fraction had antidiarrheal activity, but the antidiarrheal activity of *n*-butanol was much higher than that of the ethyl acetate fraction, which may be due to the more main active components in the *n*-butanol fraction. In this regard, we used HPLC-ESI-MS to perform a principal component analysis on this fraction, and the results showed that iridoid glycosides accounted for the main part. The previous work has revealed that iridoid glycosides had a therapeutic effect on colitis by increasing the expression of tight junction proteins (TJs) and reducing the expression of proinflammatory cytokines.¹³ The results of the study revealed that PSE extract had a therapeutic effect on rheumatoid arthritis by reducing inflammation-related microorganisms by regulating intestinal flora and significantly reducing the level of inflammatory factors in the serum of mice.⁹ However, whether

PSAE has an effective therapeutic effect on diarrhea has yet to be published.

As a new approach, network pharmacology integrates multiple platforms and technologies to explore the correlation between component targets and diseases in traditional Chinese medicine preparations by establishing multiple network models and explaining their mechanisms of action.¹⁹ In the above study, PSNB was found to contain a variety of active ingredients. Based on the hub nodes–compound network, the Venn diagram showed that PSNB had 57 targets related to diarrhea, indicating that PSNB may play a protective role against diarrhea. The network diagram of the target interaction shows that EGFR, TNF, and AKT1 are the mutual core of the network. KEGG pathway analysis showed that the mechanism of PSNB treatment of diarrhea may be highly related to non-small cell lung cancer, EGFR tyrosine kinase inhibitor resistance, HIF-1 signaling pathway, and PI3K/AKT signaling

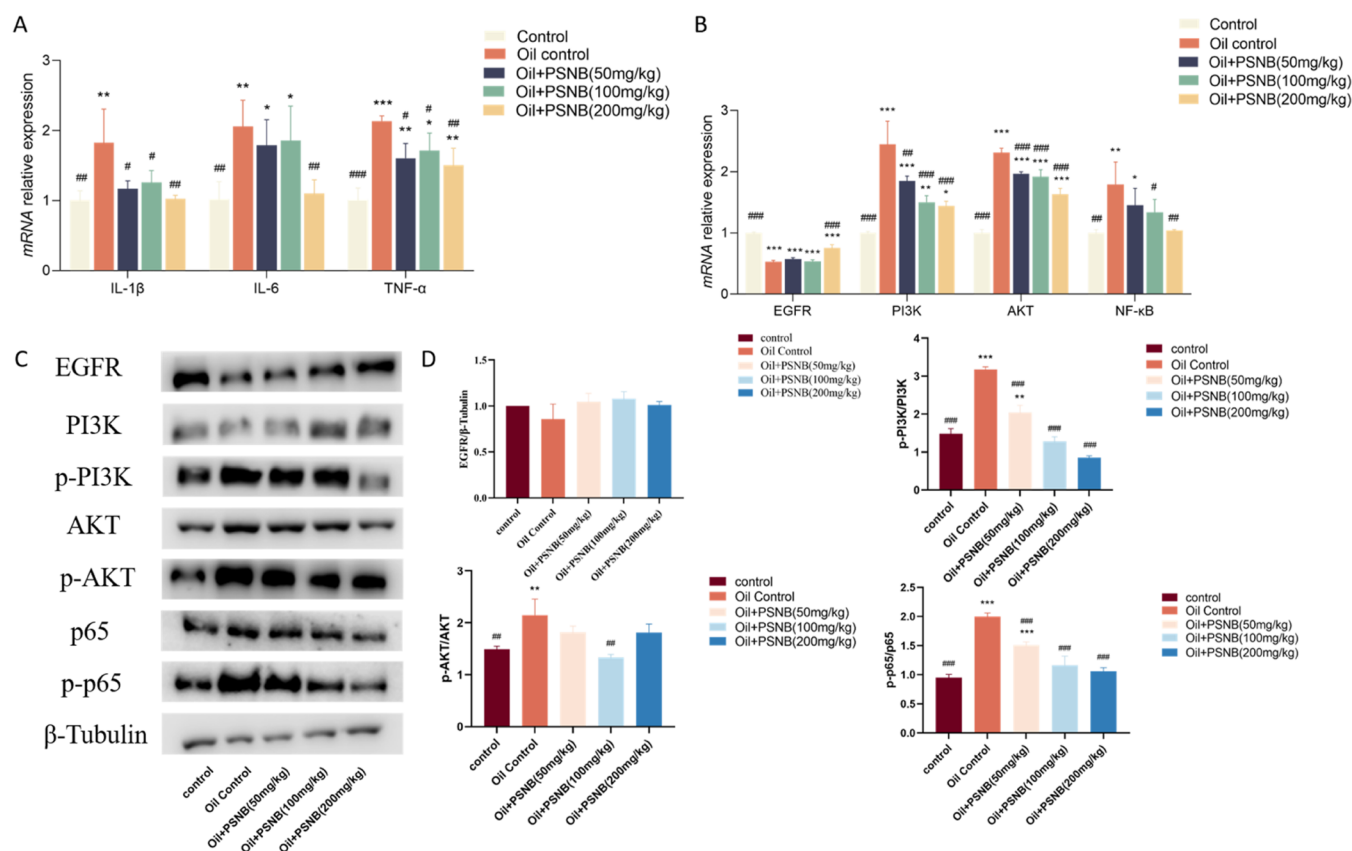


Figure 5. Effects of PSNB on the inflammatory factor and PI3K/Akt/NF- κ B signaling pathway in the small intestine of diarrheal mice. (A) Expression of the inflammatory factor mRNA level determined by real-time PCR analysis. (B) Expression of EGFR, PI3K, AKT, and NF- κ B mRNA levels determined by real-time PCR analysis. (C) Protein level of the PI3K/Akt/NF- κ B signaling pathway determined by western blotting analysis. (D) Relative protein level of the PI3K/Akt/NF- κ B signaling pathway determined by western blotting analysis. The bars represent the means, and each symbol represents an individual view. Data are presented as the mean \pm SD. The symbol for the significance of differences between the control group and another group: * P < 0.05, ** P < 0.01, *** P < 0.001. The symbol for the significance of differences between the oil control group and another group: # P < 0.05, ## P , #### P < 0.001.

Table 6. Detailed Molecular Docking Results of Ten PSNB Compounds with EGFR, AKT1, and PIK3CA

Compound	EGFR	AKT1	PIK3CA
asperuloside	-8.2	-8.4	-6.6
deacetylasperulosidic acid	-6.6	-7.3	-5.8
paederosidic acid	-7.3	-7.9	-6.2
scandoside	-6.9	-7.7	-5.1
paederoside	-7.8	-8.3	-7.0
asperulosidic acid	-7.4	-7.9	-6.3
methyl deacetylasperulosidate	-6.5	-7.7	-5.9
cleomiscosin D	-6.6	-8.7	-5.9
paederosidic acid methyl ester	-7.3	-8.0	-6.4
6'-O-E-feruloylmonotropein	-8.3	-9.8	7.6

pathway. However, the bioinformatic data currently used for targeted prediction may only reflect correlations rather than modulation of biological activity. Therefore, it is necessary to verify the action and mechanism of the action of the potential active substance utilizing appropriate tests.

EGFR is a transmembrane glycoprotein that was isolated after the discovery of its ligand EGF in 1962.^{20,21} EGFR can play a role in the repair of the small intestinal mucosa by promoting the restoration of intestinal cell proliferation and the regeneration of mucosal epithelial cells after injury.^{22,23} In our study, we observed that the inhibitory effect of EGFR in

diarrheal mice was significantly reduced after PSNB treatment, suggesting that the anti-diarrheal mechanism of PSNB may be related to the morphological and structural integrity of the mucosa involved in the EGFR gene. It has been previously demonstrated that activated EGFR recruits the downstream signal PI3K/Akt to play a key role in physiological processes such as cell proliferation, differentiation, and apoptosis. It has also been reported that PI3K/Akt is activated when diarrhea occurs.² In this study, we found that diarrhea can activate the PI3K/Akt signaling pathway, and PSNB can significantly reduce the mRNA expression of PI3K and Akt. Interestingly, at 50 mg/kg and 100 mg/kg PSNB treatment, EGFR was inhibited, but the PI3K/Akt signaling pathway was still activated. These results suggest that castor oil can lead to the activation of the PI3K/Akt cascade but not through EGFR. This result is consistent with changes in gut morphology in the group of mice treated with PSNB. According to our findings, castor oil can affect gut health and disrupt the gut barrier, and PSNB can significantly improve these conditions.

The PI3K/AKT signaling pathway also plays an important role in the development of inflammation. Activation of the PI3K/AKT pathway can increase the production of MMP through several downstream targets, of which NF- κ B is considered a key regulator,^{24,25} and activation of NF- κ B can lead to the release of different types of inflammatory factors, ultimately causing intestinal inflammation.²⁶ In addition, upon

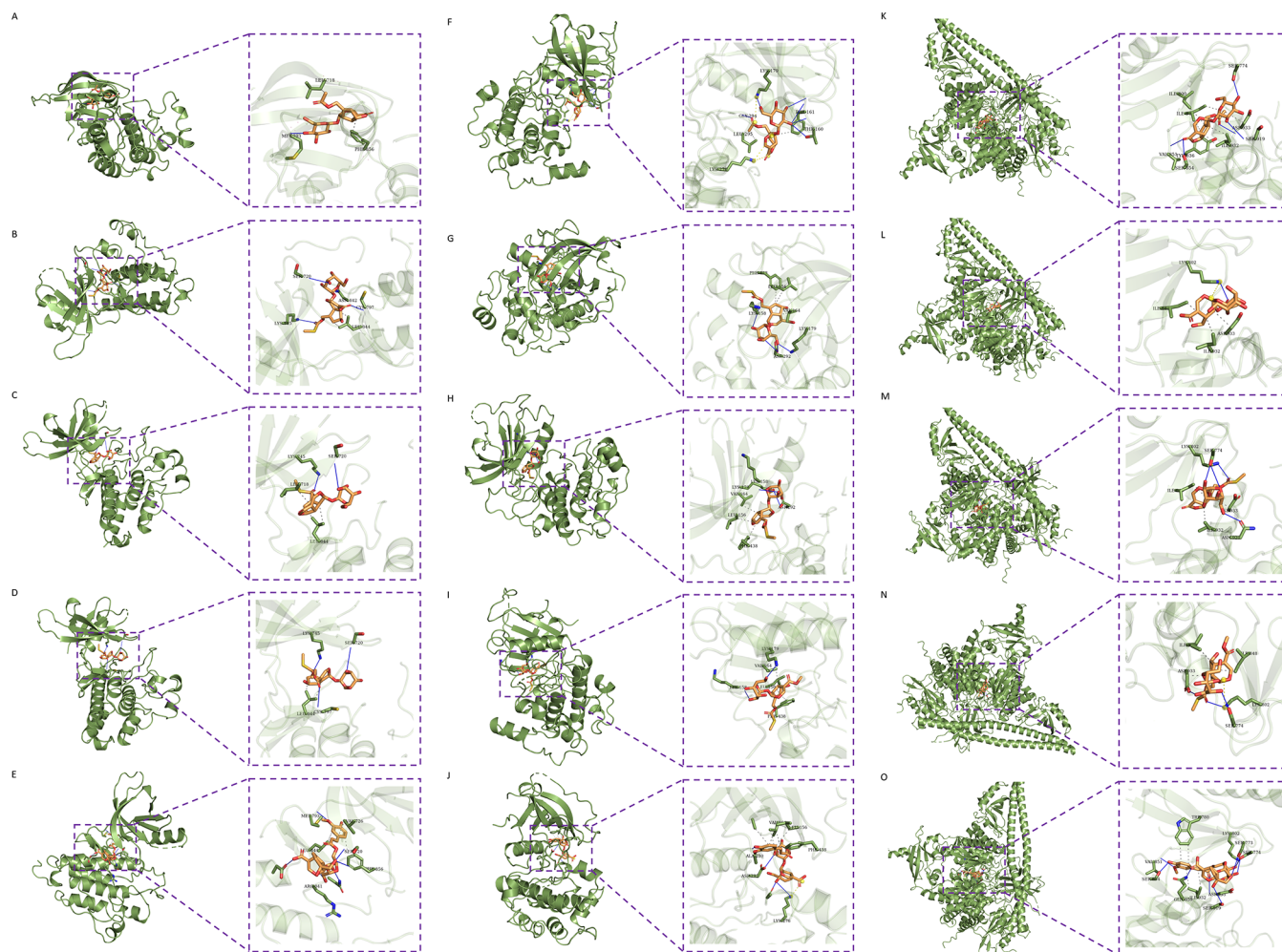


Figure 6. Bioactive components of PSNB docked to diarrhea targets. The molecular docking of asperuloside (A), paederosidic acid (B), paederoside (C), paederosidic acid methyl ester (D), and 6'-O-E-feruloylmonotropein (E) with EGFR; asperuloside (F), paederosidic acid (G), paederoside (H), paederosidic acid methyl ester (I), and 6'-O-E-feruloylmonotropein (J) with AKT1; and asperuloside (K), paederosidic acid (L), paederoside (M), paederosidic acid methyl ester (N), and 6'-O-E-feruloylmonotropein (O) with PIK3CA (G, H, I) is shown. The figure on the left shows that the compounds are located in the binding pocket of the protein. The figure on the right shows the binding sites of the compounds and proteins.

stimulation of cytokine receptors and other receptors, the membrane protein PI3K can directly or indirectly induce phosphorylation of AKT, which, in turn, activates NF- κ B.²⁴ In this study, the mRNA expression levels of PI3K, Akt, and NF- κ B increased notably in the oil control group, and the phosphorylation levels were upregulated; however, the mRNA and phosphorylation levels of PI3K, AKT, and NF- κ B were significantly decreased by PSNB treatment. In addition, the expressions of proinflammatory factors IL-1 β , IL-6, and TNF- α were also decreased to varying degrees due to the effect of PSNB. Therefore, PSNB may attenuate the inflammatory response in mice with diarrhea by inhibiting the PI3K/Akt/NF- κ B signaling pathway.

The antidiarrheal effect of PSNB was verified by network pharmacology and experimental studies. However, there is still a lack of research on the active ingredients of antidiarrheal effects. Therefore, computer-aided prediction was carried out and further predicted by molecular docking. Molecular docking results showed that asperuloside, paederosidic acid, paederoside, paederosidic acid methyl ester, and 6'-O-E-feruloylmonotropein were stably bound to the key targets identified by network pharmacology. Therefore, we speculate that asperulo-

side, paederosidic acid, paederoside, paederosidic acid methyl ester, and 6'-O-E-feruloylmonotropein may be the key components of PSNB to exert the antidiarrheal effect.

Through the enrichment analysis of the target biological process, the potential mechanism of action of PSNB on diarrheal mice was predicted, and our experiments also confirmed this mechanism, further confirming the therapeutic effect of PSNB on diarrhea.

4. MATERIALS AND METHODS

4.1. Plant Collection. The root of *P. scandens* (Lour.) Merr. was collected from Beihai City, Guangxi Zhuang Autonomous Region, China, in September 2020 and was authenticated by Dr. Junkai Wu (Heilongjiang University of Traditional Chinese Medicine). A voucher specimen (No. 21-1129.) has been deposited in the College of Veterinary Medicine, Northeast Agricultural University.

4.2. Chemicals. Acetonitrile for HPLC was acquired from Merck, and all solvents utilized for HPLC analysis were of HPLC grade (Darmstadt, Germany). Carlo Erba donated formic acid (85% v/v) (Milan, Italy). Using a Millipore Milli-Q plus system, water was filtered (Milford, MA). From Waters

Co., a PTFE membrane filter (0.45 mm) was bought (Milford, MA). All additional chemicals utilized in this investigation were obtained from Komil Chemical Reagents Co. Ltd. and were of the analytical reagent quality (Tianjin, China). Tubulin, AKT, and phospho-AKT antibodies were purchased from Abmart Shanghai Co., Ltd. PI3K, NF- κ B p65, phospho-NF- κ B p65, and EGFR antibodies were purchased from Wanleibio Shenyang Co., Ltd.

4.3. Extraction and Fractionation of *P. scandens*. *P. scandens* (500 g) was double boiled in distilled water (5000 mL) for 60 min while being stirred continuously. The resulting combined solutions were run through filter paper for filtration. To obtain 117.05 g of *P. scandens* aqueous extract, the filtrate was evaporated under reduced pressure (PSAE). The aqueous extract (100 g) was suspended in water before being fractionated with successive amounts of ethyl acetate (EA) and *n*-butanol (*n*-BuOH) to produce *P. scandens* ethyl acetate extract (3.77 g; PSEA), *P. scandens n*-butanol extract (31.51 g; PSNB), and *P. scandens* residual water extract (64.52 g; PSRW).

4.4. Experimental Animals. Adult Wister rats (180–220 g) and ICR mice (18–24 g) were purchased from the Laboratory Animal Center of Heilongjiang University of Traditional Chinese Medicine (Harbin, China). Animals were kept in standard laboratory conditions in an experimental animal room with a 12-h light/12-h dark cycle for approximately one week until the experiment. All of the experiments were approved by the Institutional Animal Ethical Committee of Northeast Agricultural University (No. SRM-08).

4.5. Acute Toxicity Assessment. ICR mice were randomly divided into four groups, each containing five mice, and different doses (0, 2000, 4000, and 5000 mg/kg) of PSAE were orally administered to groups of mice. Symptoms within 3 h and mortality within 48 h of mice were recorded. The method described by Lorke was employed.²⁷

4.6. Antidiarrheal Activity. **4.6.1. Castor Oil-Induced Diarrhea in Mice.** This model was studied according to Dong et al.²⁸ and Sheng et al.²⁹ Fasting for 18 h before starting the experiment, the mice were randomly divided into five groups (six per group). The control group was given 0.2 mL of water, the positive group received loperamide hydrochloride (5 mg/kg), and the other three groups were treated with PSAE (100, 200, and 400 mg/kg). 0.2 mL of castor oil was administered to mice after 1 h of treatment. Then, the time to first diarrhea and the total number of loose stools were observed within 4 h, and the loose stool inhibition rate was calculated by the method of Dong et al.²⁸

4.6.2. Castor Oil-Induced Intestinal Transit in Mice. In this work, the techniques described by Ahmad et al.³⁰ and Mo et al.³¹ were applied. Thirty mice were starved for 18 h before being randomly divided into five groups of six mice each. Oral doses of distilled water, loperamide (5 mg/kg), PSAE (100 mg/kg), PSAE (200 mg/kg), and PSAE (400 mg/kg) were administered to the mice in groups 1, 2, 3, 4, and 5 accordingly. Each mouse received 0.5 mL of a charcoal meal (5% acacia, 10% activated charcoal dispersion) 30 min after treatment. The mice were slaughtered, and their abdomens were dissected 30 min after receiving charcoal. The dissected mice's small intestines were immediately removed from the pylorus to the cecum, and the length of time the charcoal traveled along the gut was calculated using a calibrated ruler. A peristaltic index was used to represent how far the charcoal

meal traveled in comparison to the length of the small intestine as a whole. The following formula (Di Carlo et al., 1993) was also used to compute the percentage blockage of charcoal movement:

$$\begin{aligned} & \text{Peristaltic index of charcoal meal (\%)} \\ &= (\text{distance travel by charcoal meal (cm)}) \\ & \quad / (\text{total length of the small intestine (cm)}) \times 100 \end{aligned}$$

4.6.3. Castor Oil-Induced Enterpolling in Rats. The Bezerra et al. method was used to measure the buildup of intraluminal fluid.³² Five sets of six starved rats each were created. Treatments with distilled water, loperamide (5 mg/kg), and PSAE (100, 200, and 400 mg/kg) were administered to several groups. The aforementioned treatments were administered 1 h before giving 1 mL of castor oil orally. The rats were killed 2 h later, and the small intestine was cut out by ligating it at the ileocecal and pyloric junctions. By milking the intestinal contents into a graduated tube, the volume of the contents was measured.

4.7. Screening and Analysis of the Antidiarrheal Fraction. **4.7.1. Screening of the Antidiarrheal Fraction.** A total of 66 mice were divided into 11 groups (six mice per group). Treatments were with distilled water, loperamide (5 mg/kg), PSEA (50, 100, and 200 mg/kg), PSNB (50, 100, and 200 mg/kg), and PSAR (50, 100, and 200 mg/kg), respectively. In addition, other experimental steps are the same as in 2.6.1.

4.7.2. Analysis of the Main Compounds in the *n*-Butanol Fraction. HPLC-ESI-MS was conducted on an Ultimate 3000 UHPLC-Q Exactive (Thermo Scientific). 4 mg of *n*-butanol fraction was dissolved in methanol and filtered through a 0.22 μ m microporous membrane, and chromatographic separation of the *n*-butanol fraction was conducted using a reversed-phase Eclipse Plus C18 (100 mm \times 4.6 mm, 3.5 μ m). The mobile phase consisted of 0.1% formic acid in water (solvent A) and acetonitrile (solvent B) with a gradient program (0–2 min, B 5%–5%; 2–17 min, B 5%–95%; 17–24 min, B 95%–95%; 24–25 min, B 95%–5%; 25–30 min, B 5%–5%) at a flow rate of 0.6 mL/min. The main compounds were detected by their UV absorbance (A) at 238 nm at room temperature. The injection volume is 10 μ L. Mass spectra in the negative and positive ionization mode were generated under the following conditions: capillary temperature, 320 $^{\circ}$ C; sheath gas flow, nitrogen at 40 mL/min; auxiliary gas temperature, 300 $^{\circ}$ C; auxiliary gas flow, nitrogen at 10 mL/min; positive ion spray voltage is 3.8 kV; negative ion spray voltage is 2.8 kV; scan mode, fullms/dd-ms2 top10; primary scan range is *m/z* 10–1500 with a resolution of 70,000; secondary scan starts at 50 *m/z* with a resolution of 17,500; and collision voltage is NCE17.

4.8. Network Pharmacology Analysis. **4.8.1. Target Prediction.** Based on the basic analysis results of the above chemical substances, ten compounds were used for network pharmacological analysis to establish a compound target library, and the Swiss target online prediction website (<http://www.swisstargetprediction.ch/>) was used to forecast the target of each compound.

The disease target database DisGeNET (<https://www.disgenet.org/home/>) was used for finding diarrhea-related targets. Disease-related targets and drug component targets were entered into Venny 2.1.0 (<https://bioinfopg.cnb.csic.es/>)

Table 7. Sequences of Primers used in the RT-qPCR Analysis

gene	primer sequences	NCBI reference sequence	amplicon size (bp)
GAPDH	AAGGTCGGTGTGAACGGATT CAACAATCTCCACTTTGCCACT	NM_001289726.1	82
EGFR	TCGGGACACCCAATCAGAAA AAGGATTGCAGACGTGGTTC	NM_007912.4	84
PI3K	CGAAACAAAGCGGAGAACCTATTGC TCTACCACTACGGAGCAGGCATAG	XM_006517570.4	101
AKT1	TCAGGATGTGGATCAGCGAGAGTC AGGCAGCGGATGATAAAGGTGTTG	NM_001331107.1	108
NF- κ B	GCTACACAGGACCAGGAACAGTTC CTTGCTCCAGGTCTCGCTTCTTC	NM_001402548.1	192
IL-1 β	GCAGAGCACAAAGCCTGTCTTCC ACCTGTCTTGGCCGAGGACTAAG	NM_008361.4	198
IL-6	AGGAGTGGCTAAGGACCAAGACC CTGACCACAGTGAGGAATGTCCAC	NM_001314054.1	142
TNF- α	GCGACGTGGAAGTGGCAGAAG GCCACAAGCAGGAATGAGAAGAGG	NM_001278601.1	103

tools/venny/) to obtain potential targets for compounds acting on a diarrheal disease point.

4.8.2. Protein–Protein Interaction. Using the string platform (<https://string-db.org>), with a confidence greater than 0.7, the known therapeutic targets of diarrhea were mapped to the active component action targets of PSNB and the protein–protein interaction (PPI) was constructed, and the visualization software Cytoscape 3.8.0 was used to construct the network interaction diagram of oregano compound target diarrhea.

4.8.3. Gene Ontology (GO) and Kyoto Encyclopedia of Genes and Genomes (KEGG) Enrichment Analyses. The screened co-targets were uploaded to the DAVID bioinformatics resource database (<https://david.ncifcrf.gov/>), and Metascape (<http://metascape.org/gp/index.html>) was used to perform the GO (Gene Ontology) biological process (BP) on the co-target genes. Cellular components (CC) and molecular function (MF) enrichment analysis and KEGG (Kyoto Encyclopedia of Genes and Genomes) signaling pathway enrichment analysis were performed using Cytoscape 3.8.0 to generate the compound–target–pathway interaction network.

4.8.4. Network Construction. Ten compounds and their targets, diarrhea-related targets, and KEGG main signal pathways involved in co-target genes were uploaded to Cytoscape 3.8.0 software to construct the key compound diarrhea target KEGG signal pathway network.

4.9. Effects of PSNB on Diarrheal Mice. **4.9.1. Establishment of the Mice Diarrhea Model and Animal Administration.** After 18 h of starvation, thirty mice were randomized into five groups at random (six per group). The control group received 0.2 mL of water, as did the oil control group, while the other three groups received PSNB treatments of 50, 100, and 200 mg/kg. After 1 h of therapy, all mice except those in the control group received 0.2 mL of castor oil. All animals underwent a laparotomy to remove the ileum after 1 h of castor oil gavage on the seventh day following 7 days of continuous gavage. The tissue was divided into two sections: one was fixed in 4% paraformaldehyde for tissue sectioning and the other was snap-frozen and stored at 80 °C.

4.9.2. Histopathological Analysis. These tissues were fixed in 4% paraformaldehyde, embedded in paraffin, and sliced into 4 μ m thick slices.²⁹ These small slices were each H&E-stained.

Histopathological changes were observed with light microscopy. Villi changes, ulceration, and inflammatory processes were used to categorize tissue lesions in the colon.

4.9.3. Quantitative Real-Time PCR (qRT-PCR). The qRT-PCR analysis was carried out as previously described.³³ GAPDH were used as housekeeping genes for mRNA. Relative mRNA expression was calculated by the $2^{-\Delta\Delta C_t}$ method. The gene primer sequences are shown in Table 7.

4.9.4. Western-Blot Analysis. The small intestine was lysed with lysis buffer with a 1% protease inhibitor cocktail to harvest total cellular protein. The concentration of the extracted protein was quantified by the bicinchoninic acid (BCA) protein assay kit (Beyotime). An equal amount of the protein sample was loaded on sodium dodecyl sulfate-polyacrylamide gel electrophoresis gel and then transferred to a polyvinylidene difluoride membrane (Millipore, Billerica, MA). After the membrane was blocked with skimmed milk, it was incubated with appropriate primary antibodies. The next day, secondary antibodies conjugated with horseradish peroxidase were probed for 2–3 h. Protein signals were detected with an enhanced ECL chemiluminescence reagent based on the manufacturer's instructions.

4.10. Molecular Docking Studies. In order to predict the main useful components of PSNB for antidiarrheal effects, the interaction model of core target proteins and PSNB compounds was studied by molecular docking. The 3D structure of the compound and the X-ray crystal structure of the target protein (EGFR, PDB ID: 5UG9; AKT1, PDB ID: 4GV1; PIK3CA, PDB ID: 5XG1) were obtained from the PubChem database (<https://pubchem.ncbi.nlm.nih.gov/>) and the RCSB protein database (<http://www.rcsb.org>), respectively. Docking was performed after processing the macromolecular structure using AutoDock vina 1.1.2. The specific binding sites and atomic distances between the active ingredient and the protein were determined by the PLIP website (<https://plip-tool.biotech.tu-dresden.de/plip-web/plip/index>), and the PLIP results were used the pymol software plotted.

4.11. Statistical Analysis. Data were collected from three independent experiments and subjected to a one-way analysis of variance (ANOVA) using SPSS 22.0. Data are presented as the mean \pm standard deviation (SD). $P < 0.05$ is considered as the statistically significant difference.

5. CONCLUSIONS

PSNB has a good therapeutic effect on diarrheal mice. Through the network pharmacology method, qRT-PCR, and western-blot experiments, it was found that PSNB may reduce the inflammatory response and play an antidiarrheal effect by regulating the PI3K/Akt/NF- κ B signaling pathway. The results of molecular docking analysis showed that the antidiarrheal active ingredients in PSNB may be asperuloside, paederosidic acid, paederoside, paederosidic acid methyl ester, and 6'-O-E-feruloylmonotropein.

■ ASSOCIATED CONTENT

SI Supporting Information

The Supporting Information is available free of charge at <https://pubs.acs.org/doi/10.1021/acsomega.3c03887>.

MS spectra of ten compounds in PSNB (PDF)

■ AUTHOR INFORMATION

Corresponding Author

Zunlai Sheng – College of Veterinary Medicine, Northeast Agricultural University, Harbin 150030, P. R. China; Heilongjiang Key Laboratory for Animal Disease Control and Pharmaceutical Development, Harbin 150030, P. R. China; orcid.org/0000-0002-3059-022X; Email: shengzunlai@neau.edu.cn

Authors

Liwen Ai – College of Veterinary Medicine, Northeast Agricultural University, Harbin 150030, P. R. China; Heilongjiang Key Laboratory for Animal Disease Control and Pharmaceutical Development, Harbin 150030, P. R. China; orcid.org/0000-0002-1126-9676

Liyang Guo – College of Veterinary Medicine, Northeast Agricultural University, Harbin 150030, P. R. China; Heilongjiang Key Laboratory for Animal Disease Control and Pharmaceutical Development, Harbin 150030, P. R. China

Weixue Liu – College of Veterinary Medicine, Northeast Agricultural University, Harbin 150030, P. R. China; Heilongjiang Key Laboratory for Animal Disease Control and Pharmaceutical Development, Harbin 150030, P. R. China

Xuexue Xue – College of Veterinary Medicine, Northeast Agricultural University, Harbin 150030, P. R. China; Heilongjiang Key Laboratory for Animal Disease Control and Pharmaceutical Development, Harbin 150030, P. R. China

Lulu Li – College of Veterinary Medicine, Northeast Agricultural University, Harbin 150030, P. R. China; Heilongjiang Key Laboratory for Animal Disease Control and Pharmaceutical Development, Harbin 150030, P. R. China

Chunbo Gao – Heilongjiang International University, Harbin 150030, P. R. China

Complete contact information is available at: <https://pubs.acs.org/doi/10.1021/acsomega.3c03887>

Author Contributions

L.A.: Conceptualization, methodology, software, and writing—original draft preparation; L.G. and C.G.: data curation; W.L.: visualization; X.X.: supervision; L.L.: software and validation; and Z.S.: writing—reviewing and editing. All authors have read and approved the final version.

Notes

The authors declare no competing financial interest.

■ ACKNOWLEDGMENTS

This research was supported by the National Natural Science Foundation of China (Grant No.31572559) and the Science and Technology Project Founded by the Education Department of Heilongjiang Province (Grant No.LBH-Q18020). Mice images used in the figures were obtained from Scidraw.io. We thank Ethan Tyler and Lex Kravitz for the illustrations.

■ REFERENCES

- (1) Wenzl, H. H. Diarrhea in Chronic Inflammatory Bowel Diseases. *Gastroenterol. Clin. North Am.* **2012**, *41*, 651–675.
- (2) Zy, A.; Kai, Z. A.; Kang, Z. A.; et al. Huang Bai Jian Pi decoction alleviates diarrhea and represses inflammatory injury via PI3K/Akt/NF- κ B pathway: In vivo and in vitro studies. *J. Ethnopharmacol.* **2022**, No. 115212.
- (3) Bie, N.; Duan, S.; Meng, M.; et al. Regulatory effect of non-starch polysaccharides from purple sweet potato on intestinal microbiota of mice with antibiotic-associated diarrhea. *Food Funct.* **2021**, *12*, 5563–5575.
- (4) Mehmood, M. H.; Siddiqi, H. S.; Gilani, A. H. The antidiarrheal and spasmolytic activities of *Phyllanthus emblica* are mediated through dual blockade of muscarinic receptors and Ca²⁺ channels. *J. Ethnopharmacol.* **2011**, *133*, 856–865.
- (5) Chen, J.; Yang, H.; Sheng, Z. Ellagic Acid Activated PPAR Signaling Pathway to Protect Ileums Against Castor Oil-Induced Diarrhea in Mice: Application of Transcriptome Analysis in Drug Screening. *Front. Pharmacol.* **2020**, *10*, 1681.
- (6) Alhumaydhi, F. A.; Rauf, A.; Rashid, U.; et al. In vivo and in silico studies of flavonoids isolated from *Pistacia integerrima* as potential anti-diarrheal agents. *ACS Omega* **2021**, 15617–15624.
- (7) Kapadia, G. J.; Sharma, T.; et al. Inhibitory Effect of Iridoids on Epstein-Barr Virus Activation by a Short-term in vitro Assay for Antitumor Promoters. *Cancer Lett.* **1996**, 223–226.
- (8) Wang, Y.-C.; Huang, T. J. Screening of anti-*Helicobacter pylori* herbs deriving from Taiwanese folk medicinal plants. *FEMS Immunol. Med. Microbiol.* **2005**, *43*, 295–300.
- (9) Xiao, M.; Fu, X.; Ni, Y.; et al. Protective effects of ACS *Paederia scandens* extract on rheumatoid arthritis mouse model by modulating gut microbiota. *J. Ethnopharmacol.* **2018**, *226*, 97–104.
- (10) Chen, Y.-F.; Huang, Y.; Tang, W.; et al. Antinociceptive activity of Paederosidic Acid Methyl Ester (PAME) from the *n*-butanol fraction of *Paederia scandens* in mice. *Pharmacol., Biochem. Behav.* **2009**, *93*, 97–104.
- (11) Ma, Y.; Zhou, L.; Yan, H.; Liu, M. Effects of extracts from *Paederia scandens* (LOUR.) MERRILL (Rubiaceae) on MSU crystal-induced rats gouty arthritis. *Am. J. Chin. Med.* **2009**, *37*, 669–683.
- (12) Hou, S.-x.; Zhu, W.; Pang, M.; et al. Protective effect of iridoid glycosides from *Paederia scandens* (LOUR.) MERRILL (Rubiaceae) on uric acid nephropathy rats induced by yeast and potassium oxonate. *Food Chem. Toxicol.* **2014**, *64*, 57–64.
- (13) Yuan, J.; Cheng, W.; Zhang, G.; et al. Protective effects of iridoid glycosides on acute colitis via inhibition of the inflammatory response mediated by the STAT3/NF- κ B pathway. *Int. Immunopharmacol.* **2020**, *81*, No. 106240.
- (14) Niu, Y. T.; Zhao, Y. P.; Jiao, Y. F.; et al. Protective effect of gentiopicoside against dextran sodium sulfate induced colitis in mice. *Int. Immunopharmacol.* **2016**, *39*, 16–22.
- (15) Kim, Y. L.; Chin, Y. W.; Kim, J.; Park, J. H. Two new acylated iridoid glucosides from the aerial parts of *Paederia scandens*. *Chem. Pharm. Bull.* **2004**, *52*, 1356–1357.
- (16) Ren, L.; Xue, X.; Zhang, F.; et al. Studies of iridoid glycosides using liquid chromatography/electrospray ionization tandem mass spectrometry. *Rapid Commun. Mass Spectrom.* **2007**, *21*, 3039–3050.
- (17) Reynolds, I. J.; Gould, R. J.; Snyder, S. H.; et al. Loperamide: blockade of calcium channels as a mechanism for antidiarrheal effects. *J. Pharmacol. Exp. Ther.* **1984**, *231*, 628.

- (18) Akah, P. A.; And, C.; Agu, R. U. Studies on the antidiarrhoeal properties of *Pentaclethra macrophylla* leaf extracts. *Phytother. Res.* **1999**, *13*, 292–295.
- (19) Lv, X.; Xu, Z.; Xu, G.; et al. Investigation of the active components and mechanisms of *Schisandra chinensis* in the treatment of asthma based on a network pharmacology approach and experimental validation. *Food Funct.* **2020**, *11*, 3032–3042.
- (20) Cohen, S. Isolation of a mouse submaxillary gland. 1962.
- (21) Cohen, S.; Carpenter, G.; King, L. J. Epidermal growth factor-receptor-protein kinase interactions. Co-purification of receptor and epidermal growth factor-enhanced phosphorylation activity. *J. Biol. Chem.* **1980**, *255*, 4834–4842.
- (22) Dvorak, B. J. Milk Epidermal Growth Factor and Gut Protection. *J. Pediatr.* **2010**, *156*, S31–S35.
- (23) Nair, R. R.; Warner, B. B.; Warner, B. W. Role of Epidermal Growth Factor and Other Growth Factors in the Prevention of Necrotizing Enterocolitis. *Semin. Perinatol.* **2008**, *32*, 107–113.
- (24) Cheng, X.; Cao, Z.; Luo, J.; et al. Baicalin ameliorates APEC-induced intestinal injury in chicks by inhibiting the PI3K/AKT-mediated NF- κ B signaling pathway - ScienceDirect. *Poultry Sci.* **2021**, DOI: 10.1016/j.psj.2021.101572.
- (25) Yu-Qin, Q.; Zhen-Hua, F.; et al. Downregulating PI3K/Akt/NF- κ B signaling with allicin for ameliorating the progression of osteoarthritis: in vitro and vivo studies. *Food Funct.* **2018**, *9*, 4865–4875.
- (26) Rahmani, F.; Asgharzadeh, F.; Avan, A.; et al. Rigosertib potently protects against colitis-associated intestinal fibrosis and inflammation by regulating PI3K/AKT and NF- κ B signaling pathways. *Life Sci.* **2020**, *249*, No. 117470.
- (27) Lorke, D. A new approach to practical acute toxicity testing. *Arch. Toxicol.* **1983**, *54*, 275–287.
- (28) Dong, C. L.; Qin, Y.; Ma, J. X.; et al. The Active Ingredients Identification and Antidiarrheal Mechanism Analysis of *Plantago asiatica* L. Superfine Powder. *Front. Pharmacol.* **2021**, *11*, No. 612478.
- (29) Sheng, Z.; Yan, X.; Zhang, R.; et al. Assessment of the antidiarrhoeal properties of the aqueous extract and its soluble fractions of *Chebulae Fructus* (*Terminalia chebula* fruits). *Pharm. Biol.* **2016**, *54*, 1847–1856.
- (30) Ahmad, M.; Zezi, A.; Anafi, S.; et al. Mechanisms of antidiarrhoeal activity of methanol leaf extract of *Combretum hypopilinum* diels (combretaceae): Involvement of opioidergic and (α and β)-adrenergic pathways. *J. Ethnopharmacol.* **2021**, *269*, No. 113750.
- (31) Mo, L.; Zeng, Z.; Li, Y.; et al. Animal study of the anti-diarrhea effect and microbial diversity of dark tea produced by the Yao population of Guangxi. *Food Funct.* **2019**, *10*, 1999–2009.
- (32) Bezerra, F. F.; Cruz, L. G.; de Sousa, N. A.; et al. Antidiarrheal activity of a novel sulfated polysaccharide from the red seaweed *Gracilaria cervicornis*. *J. Ethnopharmacol.* **2018**, *224*, 27–35.
- (33) Zhao, Y.; Ma, D.; Wang, H.; et al. Lycopene Prevents DEHP-Induced Liver Lipid Metabolism Disorder by Inhibiting the HIF-1 α -Induced PPAR α /PPAR γ /FXR/LXR System. *J. Agric. Food Chem.* **2020**, *68*, 11468–11479.